Vol. 67: 117–134, 2016
doi: 10.3354/cr01363

CLIMATE RESEARCH
Clim Res

Published February 24

Sea ice impacts on polar surface weather types in the North American Arctic

Thomas J. Ballinger[1,*], Scott C. Sheridan[2]

[1]Department of Geography, Texas State University, 601 University Drive, San Marcos, TX 78666, USA
[2]Department of Geography, Kent State University, 413 McGilvrey Hall, Kent, OH 44242, USA

ABSTRACT: Summer and autumn sea ice conditions in the Western Arctic have rapidly changed in recent years, while increases in lower tropospheric air temperature and moisture have concurrently been observed across much of the high northern latitudes during the autumn (October to December) and winter (January to March) months. However, the spatiotemporal relationships between this region's ice cover and North American climate are not particularly well understood. This study employs a synoptic climatological weather typing scheme known as the Spatial Synoptic Classification (SSC) to holistically evaluate temperature and moisture characteristics throughout the terrestrial North American Arctic (NAA) associated with the Western Arctic sea ice freeze-up dates from 1979 to 2013. Monthly climatologies and linear trends of autumn/winter-dominant SSC weather types in the region, Moist Polar (MP) and Dry Polar (DP), are assessed and statistically linked to the freeze dates. Results suggest that the MP weather types are increasing, at the expense of DP types, across much of the domain. The apparent NAA transition to MP conditions is positively correlated with the timing of the Western Arctic freeze-up, and far more MP days occur during late-freeze versus early-freeze years, especially at the most northerly weather stations. Positive near-surface temperature anomalies and northerly low-level winds across the Western Arctic Ocean during late minus early freeze years potentially connect delayed ice formation to a changing NAA climate.

KEY WORDS: Sea ice · Freeze-up · Western Arctic · Weather typing · Spatial Synoptic Classification

1. INTRODUCTION

Increases in lower tropospheric temperature and moisture have been noted across much of the North American Arctic (NAA), particularly during autumn (October to December) and winter (January to March) since 1979 (e.g. Bekryaev et al. 2010, Liu et al. 2012, Serreze et al. 2012, Cohen et al. 2014). One factor connected to high and middle latitude climatic changes is the ongoing reduction of Arctic sea ice cover (e.g. Budikova 2009, Francis et al. 2009, Serreze et al. 2009, Overland et al. 2011, Serreze & Barry 2011, Stroeve et al. 2012, Vihma 2014). Given the brevity of the sea ice record, recent research has challenged the results of previous studies that largely attribute ice pack changes to atmospheric circulation anomalies in the Northern Hemisphere (e.g. Barnes 2013, Screen & Simmonds 2013, Barnes et al. 2014). Evidence, however, is mounting that Arctic warming, partly driven by sea ice losses, is playing a substantial role in lessening the hemispheric temperature and pressure gradient, leading to weakened westerlies, and yielding increased frequencies of amplified polar jet stream patterns concurrent with more persistent, anomalous surface weather conditions across portions of North America (e.g. Overland & Wang 2010, Overland et al. 2011, 2015, Francis & Vavrus 2012, 2015, Cassano et al. 2014, Francis & Skific 2015).

*Corresponding author: tballinger@txstate.edu

Recent research has also sought to deconstruct pan-Arctic sea ice–climate relationships by exploring the impact of ice variability of individual, marginal Arctic seas on synoptic-scale climate. It has been suggested that diminished ice cover in the Barents/Kara Sea and East Siberian/Chukchi Seas during autumn and winter prompts the development of thermal highs over those respective regions, which subsequently triggers widespread ridging (troughing) of the polar jet stream and positive (negative) lower tropospheric air temperature anomalies across much of the Arctic (Northern Hemisphere middle latitudes) in the weeks to months thereafter (e.g. Cohen et al. 2014, Feldstein & Lee 2014, Liptak & Strong 2014, Mori et al. 2014, Kug et al. 2015, Overland et al. 2015).

While notable sea ice changes have taken place in the Eastern Arctic, ice cover behaviors in the Beaufort and Chukchi Seas of the Western Arctic Ocean have been especially extreme, including the massive retreat of the late summer/early autumn ice edge (Xia et al. 2014) and the greatest freeze-up delays observed in the marginal seas over the satellite era (Stroeve et al. 2014). Despite being a region of rapid environmental change, especially in recent years (Wood et al. 2013, 2015), relatively little research has examined the potential relationship between Western Arctic sea ice and high/middle latitude climates of the Northern Hemisphere, particularly involving North America. Koenigk et al. (2016) found September Beaufort along with Chukchi and Bering Sea ice areas to be positively correlated with near-surface air temperatures across much of Alaska and northern Canada during the following winter. The authors also positively associate November sea ice extent in the Beaufort Sea with subsequent winter precipitation across the coasts of high latitude North America, suggesting that the condition of the autumn ice cover plays a key role on the region's climate.

Changes in the boreal sea ice cover are often linked to synoptic-scale weather and climate through analyses of observational and/or model-derived meteorological and climatological fields, such as lower/middle tropospheric air temperatures and geopotential heights, mean sea-level pressure (MSLP), and precipitation (i.e. rain and snow measurements; e.g. Francis et al. 2009, Overland et al. 2011, Mori et al. 2014). Synoptic climatological weather-type classifications holistically categorize daily weather conditions by considering multiple meteorological variables simultaneously (Yarnal 1993), and provide an opportunity to summarize thermal and moisture conditions potentially related to Arctic climate change. One particular weather-type classification based primarily on temperature and humidity observations, the Spatial Synoptic Classification (SSC; Sheridan 2002), has been used in previous cryospheric studies to assess the impacts of snow cover on air mass (i.e. weather type) frequencies (Leathers et al. 2002), and to characterize surface weather conditions associated with multidecadal snow cover changes across much of North America (Dyer & Mote 2007). Given the notable changes in autumn Western Arctic sea ice cover in recent decades, it is appropriate to evaluate the spatiotemporal relationships between the region's ice pack and the SSC weather types observed over adjacent North America. Such research is important in order to better frame how terrestrial climate change across the North American high latitudes relates to the rapid decline of Western Arctic ice cover. This work will contribute to improved understanding of the spatial extent of sea ice-related temperature and humidity changes in the Arctic and sub-Arctic, as well as the temporal response of climate in these regions to changing patterns in the timing of sea ice freeze-up.

A new approach to studying sea ice impacts is presented here, in which the SSC dataset is used to evaluate the dominant autumn and winter (October to March) NAA weather types and their associations with Western Arctic freeze-up variability, in the period 1979 to 2013.

2. DATA AND METHODS

2.1. Freeze-up data

We calculated the Western Arctic sea ice freeze dates from 1979 to 2013 (n = 35 yr) from passive microwave satellite-derived data. This specific dataset is composed of continuous freeze-up measurements garnered from the Nimbus 7 Scanning Multichannel Microwave Radiometer, and the Defense Meteorological Satellite Program 'F family' satellite platforms hosting the Special Sensor Microwave/Imager and the Special Sensor Microwave Imager/Sounder. The details of the algorithm used to process the freeze data are described in Markus et al. (2009).

Freeze-up data are obtained at a 25 × 25 km horizontal resolution for both the Chukchi Sea (66.5 to 77.3° N, 177° E to 156.5° W) and Beaufort Sea (71.2 to 77.3° N, 156.5 to 125° W) of the Western Arctic Ocean. For this study, the sea ice domain is constrained to the Western Arctic Ocean in order to better understand how freeze-up variability, in a portion of the Arctic Ocean bordering North America,

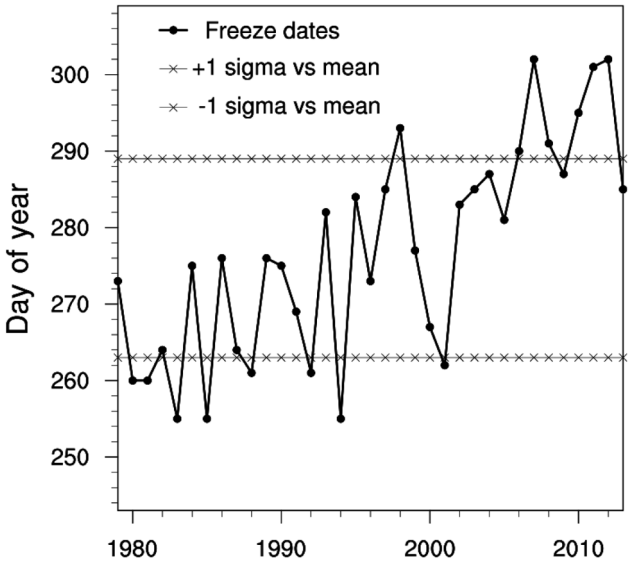

Fig. 1. Time series of annual Western Arctic freeze-up dates, 1979 to 2013. The 7 most extreme years, with respect to ±1 standard deviation (σ) from the 1981 to 2010 mean freeze-up date (day of year = 276), are used to produce the composite analyses described in Sections 3.3 and 3.4

relates to dominant NAA weather types. During the processing of the data, those pixels not registering a freeze date or intersecting a portion of the adjacent land surface are removed from the analysis. All pixels that register a freeze-up date are then averaged for each year across the respective Arctic marginal seas. The individual Beaufort and Chukchi freeze dates are then averaged together each year (1979 to 2013), yielding a cohesive time series of Western Arctic freeze-up dates, which vary between September 11/12 (day of year [DOY] 255) and October 28/29 (DOY 302) for leap/non-leap years throughout the study period (Fig. 1).

Extreme freeze-up years are identified as those that are at least ±1 standard deviation (σ) from the 1981–2010 mean freeze-up date (DOY = 276, σ = 13 d). In order to maintain symmetry in forthcoming composite analyses, the 7 most extreme positive years (1998, 2006 to 2008 and 2010 to 2012; hereafter 'late years') and negative years (1980, 1981, 1983, 1985, 1988, 1992, 1994; hereafter 'early years') are considered (Fig. 1). Freeze-up dates are after October 16/17 (DOY = 290) in late years and before September 17/18 (DOY = 261) in early years. Late minus early year composites of monthly weather type frequencies and synoptic fields are further described in Sections 2.3 and 2.4 and explored in Sections 3.3 and 3.4.

2.2. The Spatial Synoptic Classification (SSC)

The SSC weather-typing scheme is used in this study to holistically assess near-surface, *in situ* thermal and moisture characteristics across the NAA during October to March, which may be related to the temporal variability of the Western Arctic sea ice freeze-up. In total, 27 first-order weather stations (as shown in Fig. 2 and described in Table 1) north of 60° N in North America (including Greenland) possess SSC calendars that are complete from 1979 to between 2010 and 2013 (i.e. with observations terminating between 2010 and 2013).

The SSC takes into account 6-hourly surface air temperature (SAT), dew point (Td), MSLP, wind speed and direction, and cloud cover as measured at the weather stations to classify each day of the year into 1 of 7 different weather types, largely according to their temperature and moisture characteristics. These weather types include Dry Moderate, Dry Polar, Dry Tropical, Moist Moderate, Moist Polar, Moist Tropical, and Transition. Each day is identified as a particular weather type based on that day's resemblance to the climatological conditions defining the weather type for that specific time of year.

The primary weather types classified in the NAA throughout most of the year, especially during the autumn and winter months, are dry polar (DP) and moist polar (MP), and these two types represent the focus of forthcoming analyses in Section 3. DP mirrors the continental polar (cP) air mass and is associated with clear, dry, and frigid conditions in the Arctic during the aforementioned study months. MP resembles the maritime polar (mP) air mass, and is characterized by cloudy and humid weather, and higher temperatures relative to the DP type.

An example of temperature and moisture disparities by SSC type is presented in Fig. 3. November mean SATs (Tds) during MP days range from −3°C (−6°C) at Anchorage to −18°C (−21°C) at Eureka. DP classified days exhibit mean SATs (Tds) from −8°C (−14 and −15°C, respectively) at Anchorage and Talkeetna to −32°C (−37°C) at Eureka. Differences in thermal and moisture observations are therefore apparent with MP days exhibiting 4 to 14°C higher SATs and 8 to 16°C higher Tds versus days categorized as DP. It is important to note that the climatological characteristics of the MP and DP types vary across time (i.e. day-to-day) as well as space, so that in February, for example, mean conditions with both weather types are colder than those displayed for November (see data on 'Climatology – SSC Characteristics' available for each station on the SSC homepage, http://sheridan.geog.kent.edu/ssc.html).

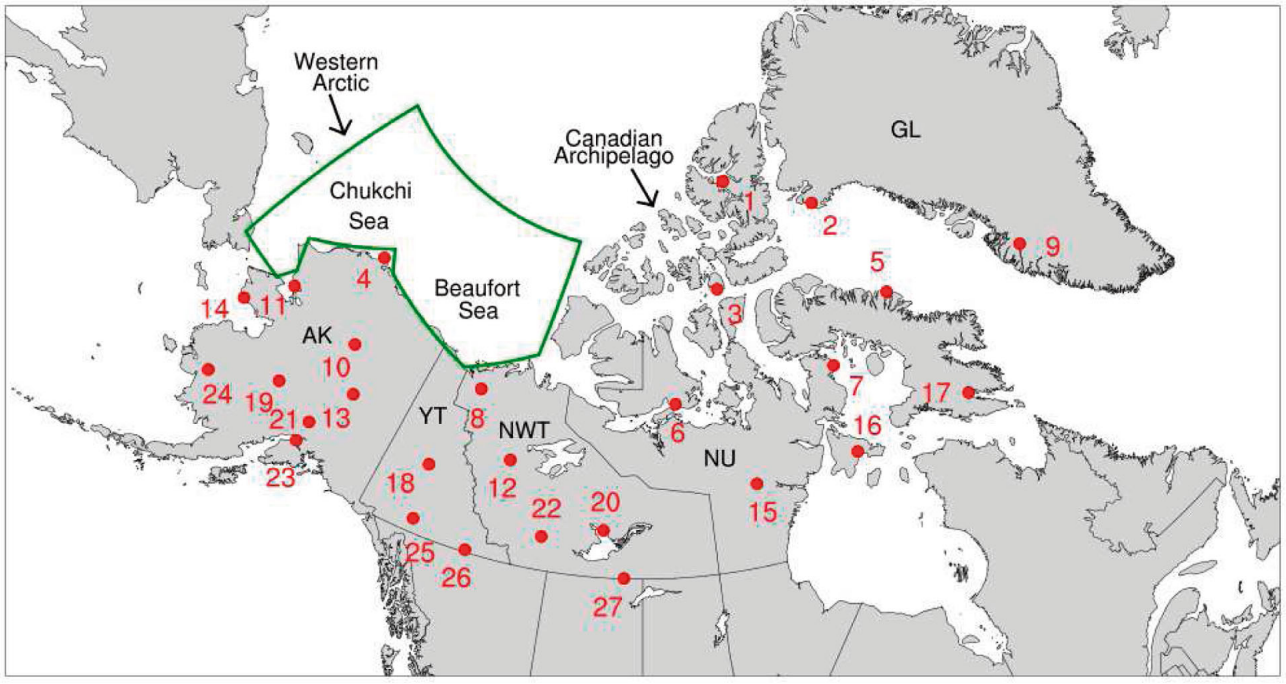

Fig. 2. North American Arctic study area comprised of 27 first-order weather stations (red dots) that possess complete Spatial Synoptic Classification calendars. Table 1 provides details on each station. The green polygon outlines the Beaufort and Chukchi Seas that collectively comprise the Western Arctic sea ice freeze-up domain

2.3. NCEP/NCAR reanalysis data

The National Centers for Environmental Prediction/National Center for Atmospheric Research (NCEP/NCAR) first generation reanalysis (Kalnay et al. 1996) monthly mean fields of 925 hPa air temperature (T_{925}) and vector winds (V_{925}), and 500 hPa geopotential heights (Z_{500}) are selected to evaluate the potential climatological mechanisms linking freeze-up patterns to the variability of terrestrial MP and DP weather types. While NCEP/NCAR reanalysis products have some deficiencies, such as short-term, positive Arctic SAT biases noted around the turn of the 20th century connected to the use of disparate sea ice products (http://www.esrl.noaa.gov/psd/data/reanalysis/problems.shtml), recent studies have utilized the T_{925}, V_{925}, and Z_{500} data, which closely follow satellite and radiosonde observations, to assess climatic changes across the boreal high and middle latitudes (e.g. Serreze et al. 2011, Wood et al. 2013, Francis & Vavrus 2015). Monthly plots (October to March) of the aforementioned fields for the domain 45 to 90° N, 150° E to 30° W are produced using NOAA's monthly/seasonal climate compositing tool (http://www.esrl.noaa.gov/psd/cgi-bin/data/composites/printpage.pl) and summarized in Section 3.4.

2.4. Descriptions of statistical analyses

The October to December MP and DP climatologies and linear trends span the period 1979–2013, while the January to March climatologies and trends are calculated over the 1980–2013 period. Further, October to December MP/DP and freeze-up correlations of the respective datasets cover a similar period, from 1979 to between 2010 and 2013, while the January to March correlations take into account the temporal offset between the observed freeze dates and the SSC data extending into the aforementioned winter months of following year. MP/DP composite analyses are limited to 22 NAA stations and exclude YRB, YFB, YZF, BET, and YXY (see Table 1 for abbreviations) because their records terminate prior to 2013, following the final late freeze year. Similar to the temporal details of the weather type and freeze-up correlation analyses previously described, the composites of NCEP/NCAR data for January to March reflect the months immediately following the observed early or late freeze-up extremes of the previous autumn.

Associations between monthly frequencies of MP and DP weather types and the freeze-up dates are conducted using correlation analysis and compositing procedures, and subsequently mapped and described in the results section. The statistical

Table 1. Details of the North American Arctic weather stations with Spatial Synoptic Classification calendars (displayed in Fig. 2) analyzed in this study. The stations are located in Alaska (AK), USA, Yukon Territory (YT), Northwest Territories (NWT), and Nunavut (NU), Canada, and Greenland (GL)

Station	Station name and location	Abbreviation	Lat (°N)	Lon (°W)	Data record
1	Eureka, NU	WEU	79.98	85.13	1979–2013
2	Thule, GL	THU	76.53	68.70	1979–2013
3	Resolute, NU	YRB	74.72	94.97	1979–2010
4	Barrow, AK	BRW	71.29	156.77	1979–2013
5	Clyde River, NU	YCY	70.48	68.52	1979–2013
6	Cambridge Bay, NU	YCB	69.10	105.13	1979–2013
7	Hall Beach, NU	YUX	68.78	81.25	1979–2013
8	Inuvik, NWT	YEV	68.31	133.50	1979–2013
9	Kangerlussuaq, GL	SFJ	67.01	50.72	1979–2013
10	Bettles, AK	BTT	66.92	151.53	1979–2013
11	Kotzebue, AK	OTZ	66.89	162.60	1979–2013
12	Norman Wells, NWT	YVQ	65.28	126.79	1979–2013
13	Fairbanks, AK	FAI	64.82	147.87	1979–2013
14	Nome, AK	OME	64.51	165.43	1979–2013
15	Baker Lake, NU	YBK	64.30	96.08	1979–2013
16	Coral Harbor, NU	YZS	64.19	83.35	1979–2013
17	Iqaluit, NU	YFB	63.75	68.54	1979–2010
18	Mayo, YT	YMA	63.62	135.87	1979–2013
19	McGrath, AK	MCG	62.95	155.60	1979–2013
20	Yellowknife, NWT	YZF	62.47	114.44	1979–2010
21	Talkeetna, AK	TKA	62.32	150.09	1979–2013
22	Fort Simpson, NWT	YFS	61.75	121.23	1979–2013
23	Anchorage, AK	ANC	61.17	150.00	1979–2013
24	Bethel, AK	BET	60.78	161.83	1979–2012
25	Whitehorse, YT	YXY	60.72	135.07	1979–2010
26	Watson Lake, YT	YQH	60.12	128.83	1979–2013
27	Fort Smith, NWT	YSM	60.02	111.95	1979–2013

strength of the relationships between the respective freeze-up data and individual month MP and DP frequency time series (from each NAA station) is assessed using Pearson bivariate correlations. Comparisons with Spearman's rank correlations were also explored, but are not presented, as the coefficients were not appreciably different than those derived using Pearson's method. Mean composites of weather type frequencies (Section 3.3) and reanalysis fields (Section 3.4) are constructed to evaluate NAA differences in the respective surface and lower-to-middle tropospheric climate conditions during extreme freeze-up years. Statistical significance is assessed with 2-tailed *t*-tests (≤0.05) in the trend, correlation, and composite analyses.

3. RESULTS

3.1. MP/DP climatology and trends

Monthly climatologies of the NAA MP and DP weather types for October to March are presented in Figs. 4 & 5. The MP weather type is the dominant type for much of the study region in October, with frequencies ≥50% of classified days for many of the western and southernmost stations in the domain (Fig. 4). Frequencies of MP days fall substantially, particularly over the northern and eastern parts of the domain, in November and December. Relatively low MP frequencies are observed from January to March, ranging from ~20% across the Canadian Archipelago to 40% towards the western and easternmost edges of the domain.

The DP weather type is more prevalent than the MP type during the cold season months (Fig. 5). With the exception of October, when mean occurrences of DP days are typically less than MP, November to March months exhibit DP frequencies between ~50 and 80% of all classified days for much of the central core of the NAA, and decrease to between ~20 and 40% of days across the southern, eastern, and western periphery during these months.

Climate changes have resulted in shifts of SSC type frequencies over time (Figs. 6 & 7). Positive trends in MP classified days (0.10 to 0.40 d yr^{-1}) are apparent in October to December and February for portions of the NAA (Fig. 6). The strongest, significant trends during these months are concentrated in north/central Alaska, portions of the Canadian Archipelago, and northwestern Greenland. Negative monthly DP trends compensate for much of the aforementioned increase in MP days since 1979 (Fig. 7). These largely offsetting DP decreases (–0.10 to –0.30 d yr^{-1}) are primarily collocated over similar NAA areas as the MP increases and represent an ongoing transition to more humid and warmer conditions in the NAA.

3.2. MP/DP and freeze-up correlations

Multidecadal interactions between MP/DP weather type variability and Western Arctic Ocean freeze-up dates are statistically evaluated in order to assess these low-frequency relationships over the study period. Initially, correlations were calculated separately between the Chukchi Sea, Beaufort Sea, and Western Arctic Ocean freeze-up dates and SSC frequencies to see if results significantly vary depending on ice domain. Few differences in the strength

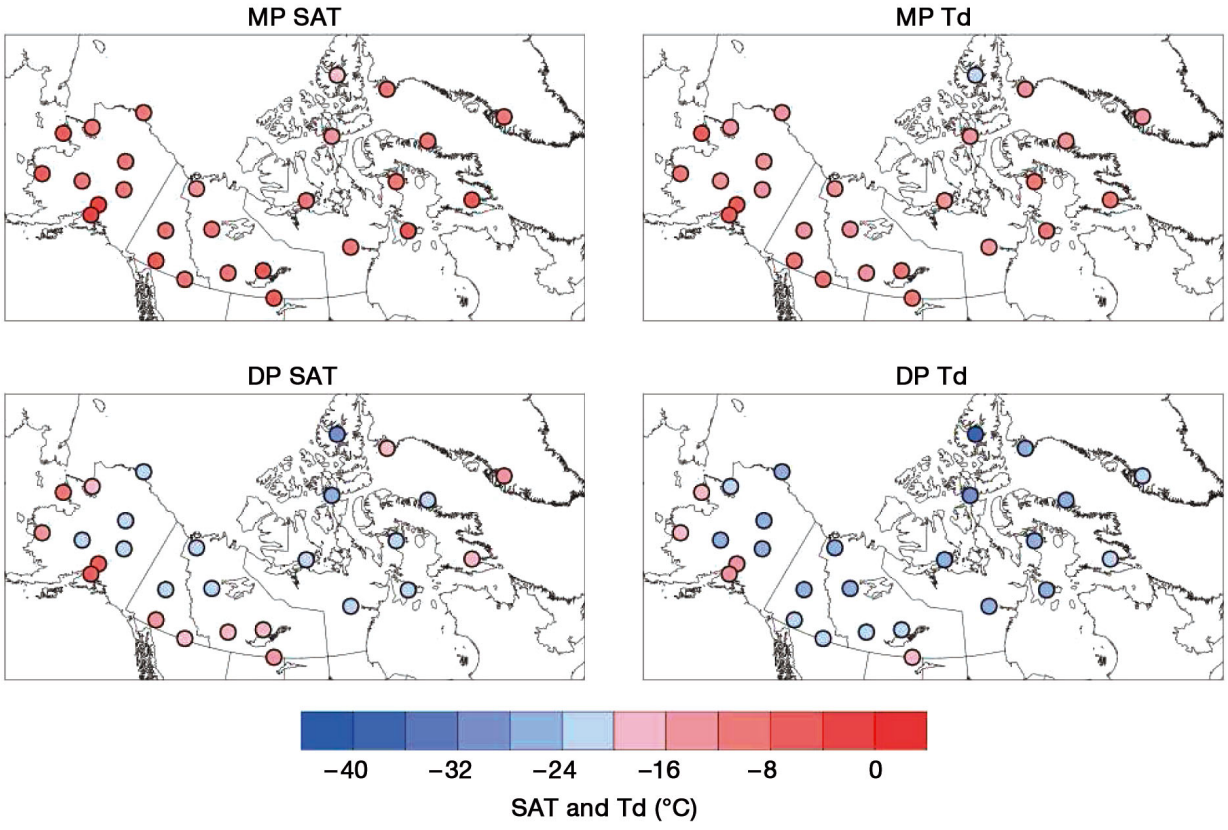

Fig. 3. Mean November surface air temperature (SAT) and dew point (Td) for the Dry Polar (DP) and Moist Polar (MP) weather types

of the correlations are observed (e.g. see Fig. S1 in the Supplement at www.int-res.com/articles/suppl/c067p117_supp.pdf), and the sign of the coefficients is consistent with each domain throughout the NAA. Therefore the broad Western Arctic domain, comprising both marginal Arctic seas, is selected for analyses in the remaining results sections.

Correlation coefficients between the monthly MP frequencies and Western Arctic freeze-up are presented in Fig. 8. Positive and statistically significant correlations consistently appear during October to December across much of the northern and western areas of the NAA. The most positive coefficients are found over northern Alaska during November (r ~ 0.50) suggesting a strong, localized relationship between the freeze onset and MP classified days along the North Slope, specifically at Barrow. The correlations generally weaken to the south and across the Canadian Archipelago as coefficients are negligible to weakly negative (r = 0.00 to −0.20) during most months with increasing distance from the Western Arctic Ocean.

DP weather types are predominantly anti-correlated with the freeze-up dates (Fig. 9). Correlation coefficient magnitudes are significant and mostly negative during October and November for several of the northernmost NAA stations (r ~−0.40 to −0.50), but the strength of the DP–freeze relationships decreases southward. Most of the NAA is otherwise characterized by weakly positive and/or negative correlations across most months. Positive DP–freeze associations are found along western Greenland (i.e. Kangerlussuaq), which together with the negative MP–freeze correlations shown in Fig. 8 suggest that this region's surface environment is becoming cooler and drier (with later Western Arctic ice cover formation) in contrast to the warming and moistening surface conditions witnessed throughout much of the NAA.

3.3. MP/DP composites

Relationships between the freeze date time series and MP/DP frequencies are further investigated by exploring the differences in these weather types' frequencies during extreme (i.e. late minus early) freeze-up years. Fig. 10 shows the mean differences in MP classified days between the late and early

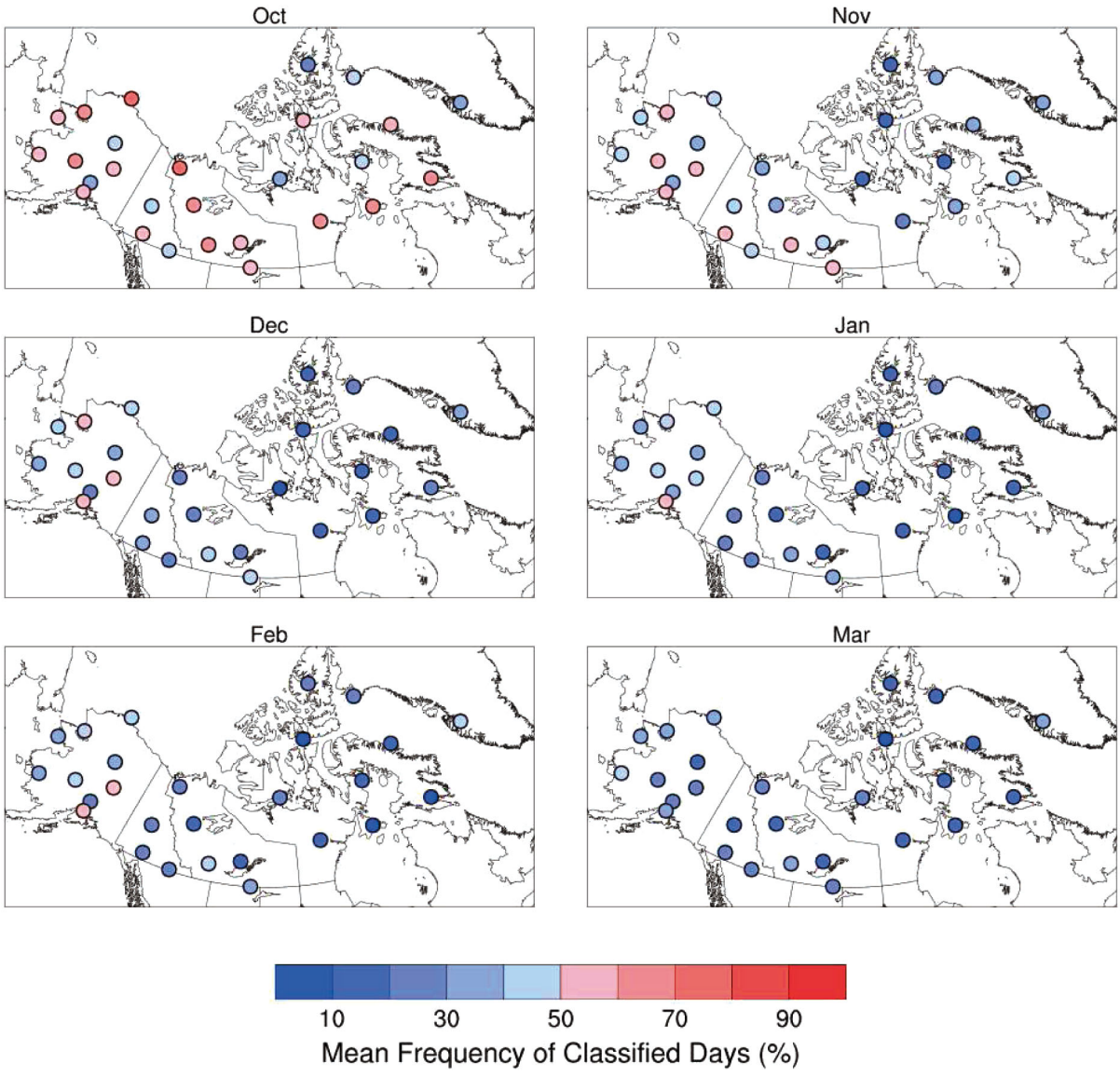

Fig. 4. Monthly mean frequencies of Moist Polar classified days for October to March

freeze years. Mean increases in MP frequencies during late-freeze years are most pronounced (2 to 8 d yr^{-1}) and spatially consistent across the Alaskan and Yukon Territory stations. In particular, Barrow during November exhibits the strongest positive difference (+8 d yr^{-1}) among the stations surveyed. Northern stretches of the Yukon and Northwest Territories and north/central Alaska also demonstrate MP changes of +2 to 6 d yr^{-1} on average during November, with more statistically-significant differences and greater positive deviations in MP classified days found in areas closer to the Western Arctic Ocean.

Anomalous differences in the DP composites generally contrast those of the MP results. For instance, DP classified days occur much less frequently in late versus early freeze years for northern Alaska (i.e. Barrow) and the southeastern Canadian Archipelago during October and especially November (Fig. 11). There is a substantial gradient of DP differences observed during November stretching from northern Alaska (–12 d yr^{-1}) to the central part of the state (+4 d yr^{-1}), suggesting an abrupt transition of thermal and moisture conditions with increasing distance from the ocean during this month that is not nearly as strong in the other autumn and winter months. Much of interior Alaska, the Yukon, and Northwest Territories show positive departures in DP classified days in November as well as March (2 to 10 d yr^{-1}), indicating cooler, drier weather types prevail in these continental locales following later freezing of the adjacent ocean surface.

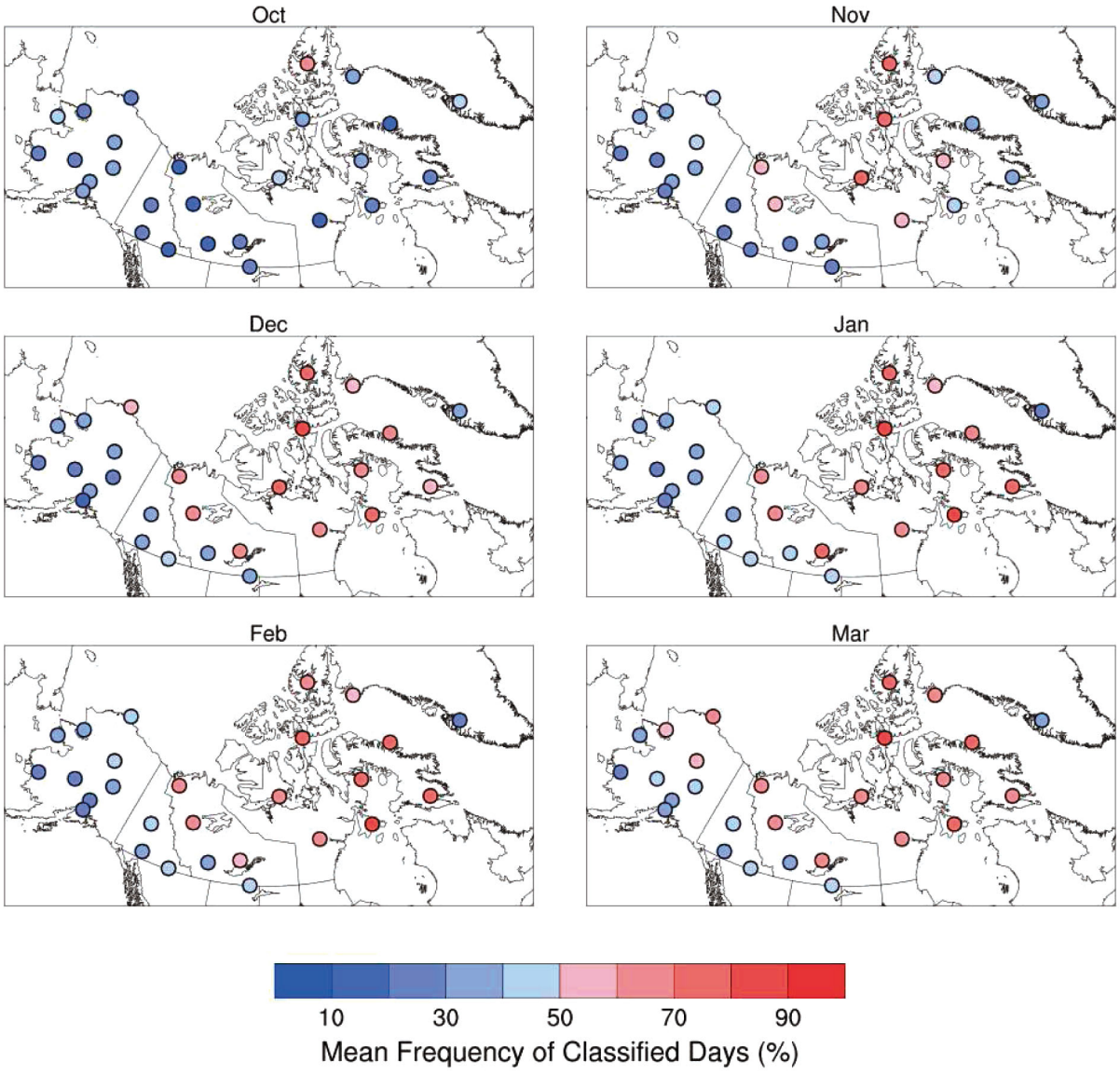

Fig. 5. Monthly mean frequencies of Dry Polar classified days for October to March

3.4. Linkages to climatic mechanisms

Composite NCEP/NCAR fields of late minus early freeze-up years reveal potential physical links between the Western Arctic freeze-up onset and NAA climate (Figs. 12 & 13). Positive T_{925} departures (1 to 4°C) characterize the low-level thermal environment over most of the Western Arctic Ocean from October to January, though the strength of the temperature anomalies wanes into the winter months. The prevailing V_{925} wind direction during these months is primarily northerly, which would suggest advection of the anomalously warm air located over the ocean onto the North American continent contributes to higher numbers of MP days across portions of Alaska, and the Yukon and Northwest Territories.

Z_{500} height differences generally support the low-level flow over the study region (Figs. 12 & 13). For example, November anomalies of +90 geopotential meters (gpm) over northeastern Siberia coincide with a steep height gradient and increased meridional flow over the Western Arctic Ocean, Alaska, and the North Pacific. The January Z_{500} composite map resembles a blocking pattern over the northernmost NAA with slightly negative height anomalies extending from the eastern Beaufort Sea through central Canada, which are bookended by anomalies of at least +60 gpm over northeastern Siberia and across most of Greenland. This ampli-

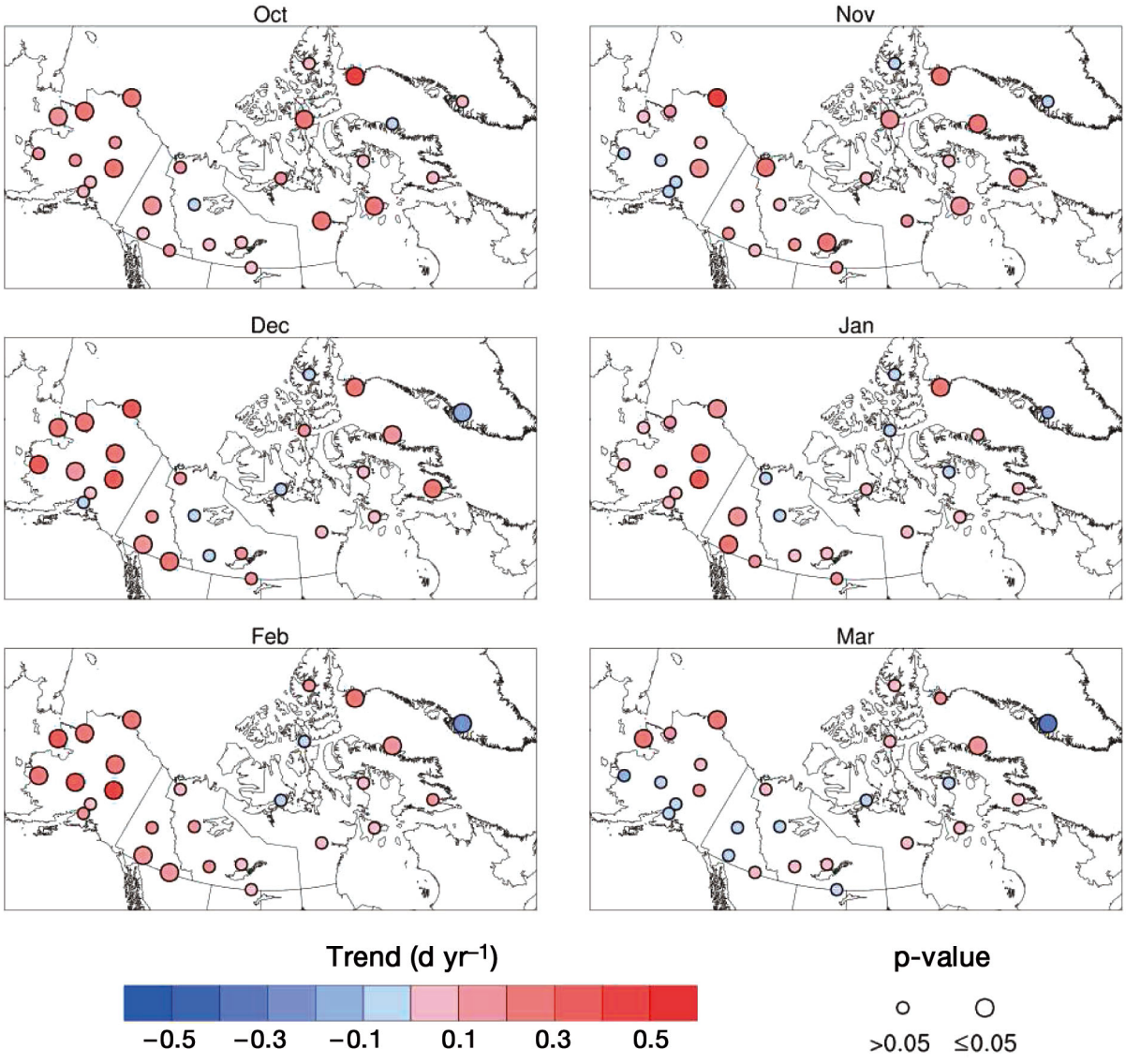

Fig. 6. Slope magnitudes and corresponding statistical significance of Moist Polar linear trends for October to March

fied Western Arctic height pattern may represent a regional component of the hemispheric-scale 500 hPa flow, often quantified by the Pacific-North American pattern (PNA; Wallace & Gutzler 1981). In order to further explore how this pattern relates to the principal NAA weather types, correlations are analyzed between the monthly (October to March) Climate Prediction Center PNA index (www.cpc.ncep.noaa.gov/products/precip/CWlink/pna/pna.shtml) and MP and DP occurrences (see Figs. S2 & S3 in the Supplement). The MP (DP) and PNA correlations are primarily positive (negative), providing further evidence of links between wavier NAA atmospheric circulation, in this case as shown in the regional composites, and relatively warm, humid NAA surface weather conditions. Thus, the anomalously warm air masses over the Western Arctic appear to be transported to the NAA by northerly V_{925} winds, which are supported by meridional mid-tropospheric flow aloft, thereby explaining a possible connection between delayed freeze conditions and the broadly observed patterns of positive MP anomalies.

4. DISCUSSION

NAA MP and DP weather type frequencies are evaluated and associated with the Western Arctic freeze-up time series and the most extreme freeze-up years over the 1979 to 2013 period. The results indi-

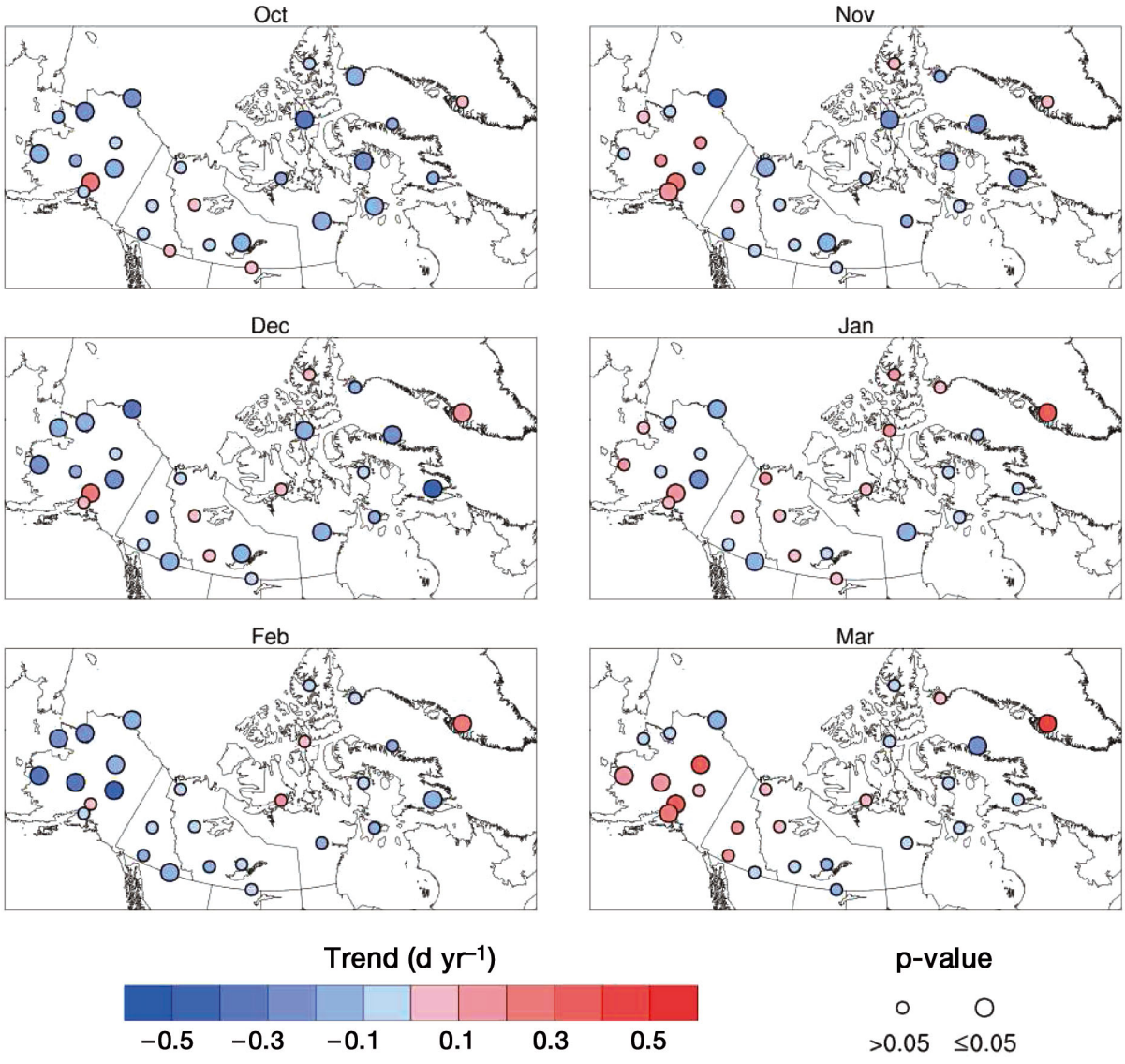

Fig. 7. Slope magnitudes and corresponding statistical significance of Dry Polar linear trends from October to March

cate that October to December and February MP (DP) weather type frequencies appear to be increasing (decreasing) rather substantially, especially across the northern and westernmost SSC stations (contrast Figs. 6 & 7). Autumn MP weather type increases at stations near the Western Arctic Ocean coastline suggest that persistence in Beaufort and Chukchi Sea ice cover formation is strongly influencing the warming and moistening of the coastal and near-coast climates over time, especially adjacent to the North Slope (e.g. Wendler et al. 2010, 2014, Serreze et al. 2012).

Relatively strong correlations between the sea-ice freeze dates and the monthly MP frequencies extend beyond stations located in close proximity to the Western Arctic Ocean during most months (Fig. 8). This link suggests that the delays in ice cover formation impact not only coastal environments, but also remote, continental locations across portions of the NAA. For most months, the highest positive correlation coefficients occur within the western half of the domain, encompassing both Alaska and the Yukon Territory. Peak coefficient magnitudes spatially vary by month within this portion of the NAA, but appear strongest over northern Alaska during November (Fig. 8). Bieniek et al. (2014) noted positive November SAT trends (1981–2012) across much of Alaska with warming maximized over the North Slope and

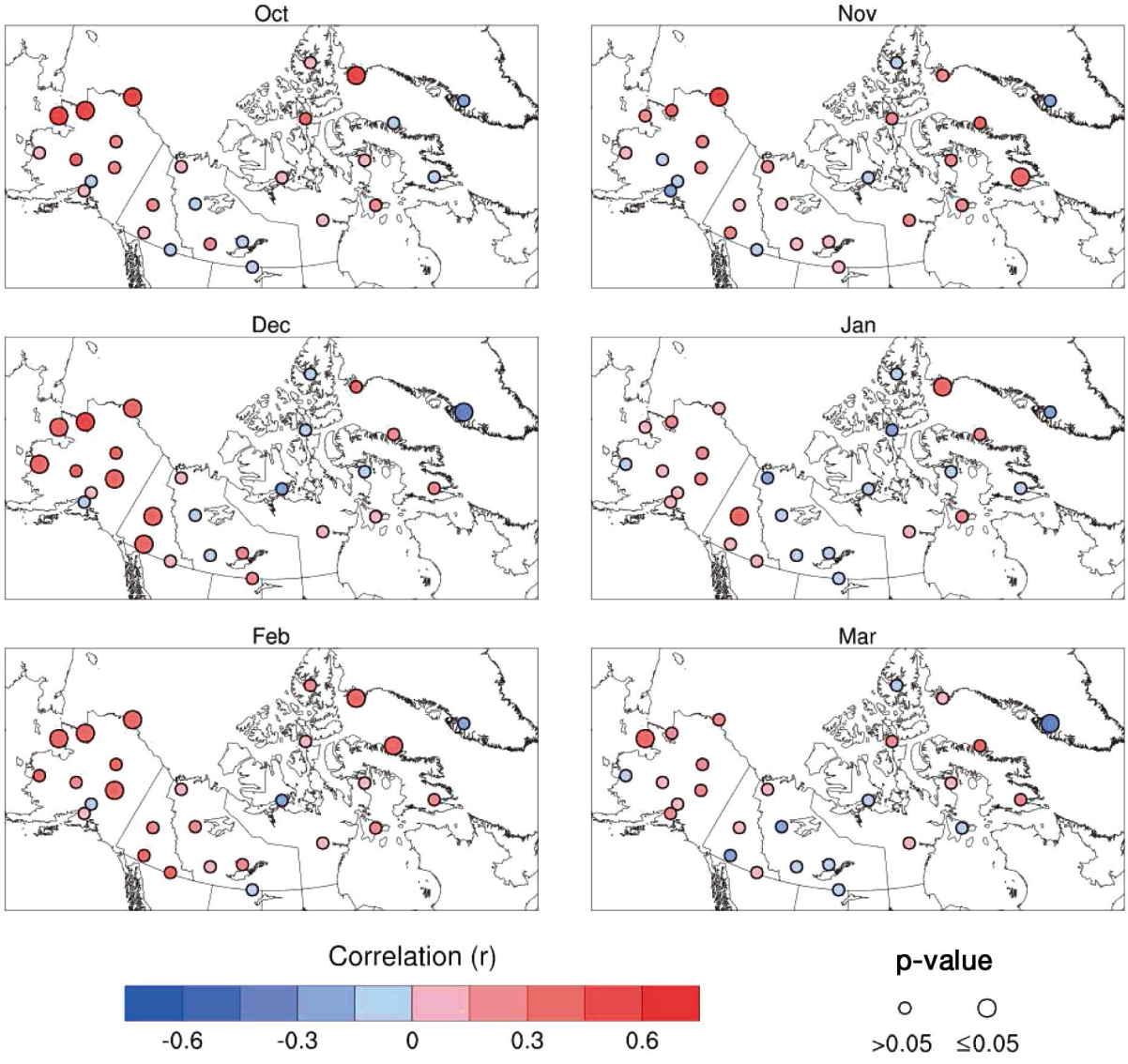

Fig. 8. Coefficient magnitudes and corresponding statistical significance of correlations between October and March Moist Polar weather type occurrences and the freeze date of Western Arctic sea ice

diminishing toward the Gulf of Alaska, which may partially explain the spatial pattern of MP associations with the ice cover.

SSC composites highlight anomalous MP/DP occurrences as MP classified days tend to occur much more often during late freeze years throughout much of the domain relative to anomalously early freeze-ups (Fig. 10). The results indicate that during the most extreme late years the increases in MP frequencies (especially across Alaska) persist through February, suggesting that the autumn freeze-up delays are, in part, leading to warmer and more humid surface conditions in the winter months. The NCEP/NCAR synoptic fields assist in physically linking these weather type changes to the ice cover, especially during November and January (Figs. 12 & 13). During late years, anomalously warm 925 hPa air over the Beaufort and Chukchi Seas tends to be advected inland by anomalous, low-level winds. The Z_{500} composites reveal positive, regional height anomalies accompanying meridional flow during late versus early freeze years. These flow composites are reminiscent of positive PNA patterns, which are shown to be directly linked to increases in cold season MP days, especially across Alaska, the Yukon, and Northwest Territories (Fig. S2 in the Supplement). This synoptic setting supports the southward dispersion of relatively warm, near-surface air over-

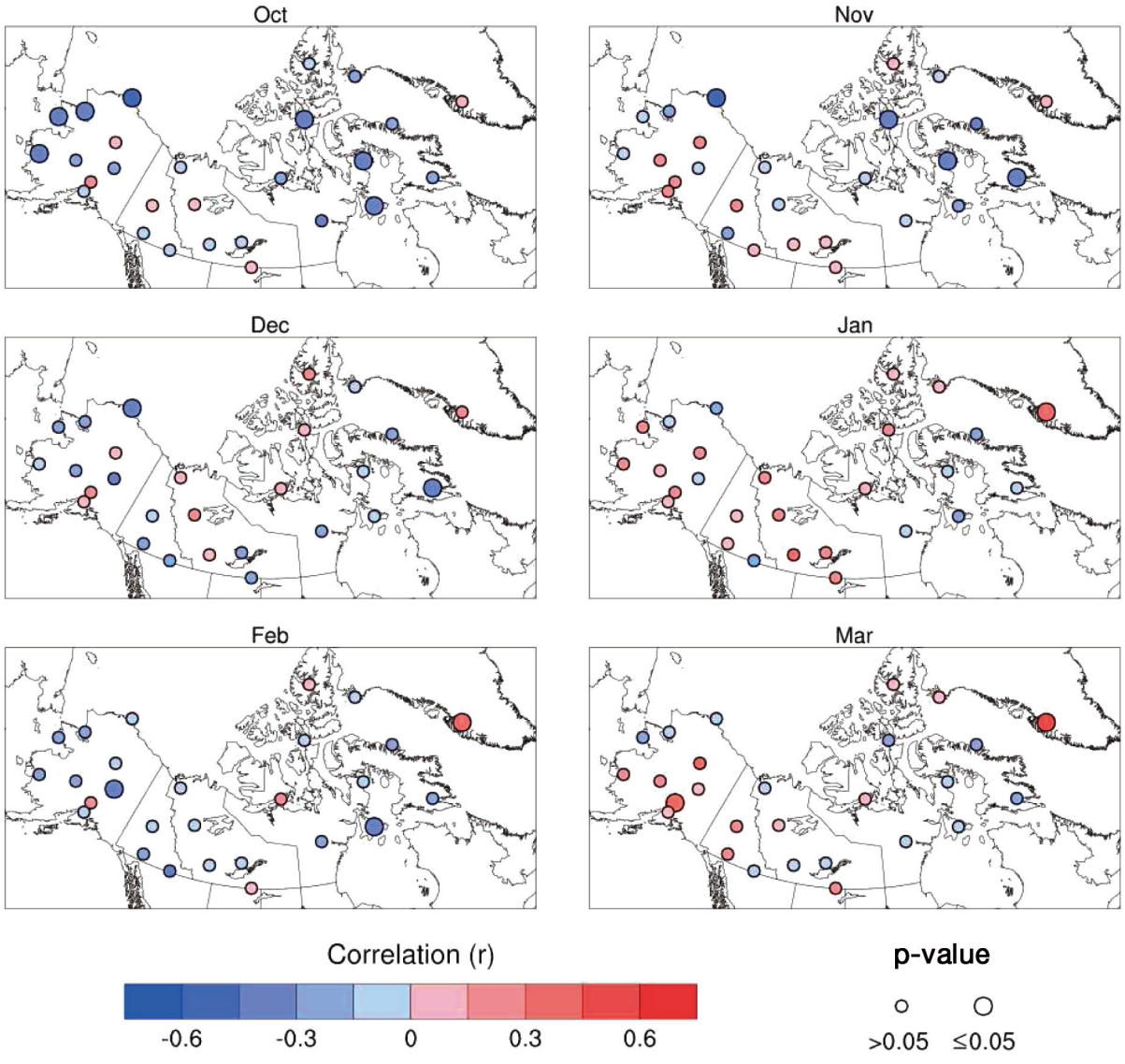

Fig. 9. Coefficient magnitudes and corresponding statistical significance of correlations between October and March Dry Polar weather type occurrences and the freeze date of Western Arctic sea ice

laying the Western Arctic Ocean to much of the NAA, and also suggests that incursions of maritime air masses from the North Pacific may also play a role in the observed frequency changes of the weather types (e.g. Liu et al. 2015).

Similar mechanisms that physically link sea ice loss and North American climatic changes are identified in recent studies. Autumn months since the late 1990s have exhibited increases of low-level, northerly wind events in the Western Arctic (Asplin et al. 2015), while occurrences of amplified 500 hPa height patterns were more common during the cold season over North America from 1995 to 2013 compared to 1979 to 1994 (Francis & Vavrus 2015). During recent autumns and winters, northerly flow across areas of declining Western Arctic sea ice concentration coincided with large swaths of positive T_{925} anomalies (~0.5 to 1.5°C) throughout the NAA (Serreze et al. 2011). Middle and lower tropospheric dynamic forcing of relatively warmer, more humid maritime air well into continental North America suggests one set of links between the anomalous ice conditions and the multidecadal transition from DP to MP conditions.

A cold season dichotomy between Arctic warming events and cold air outbreaks across the North American middle latitudes appears to be increasingly common in recent years (e.g. Overland et al. 2011, Kug et al. 2015). In this manuscript, regional freeze-up

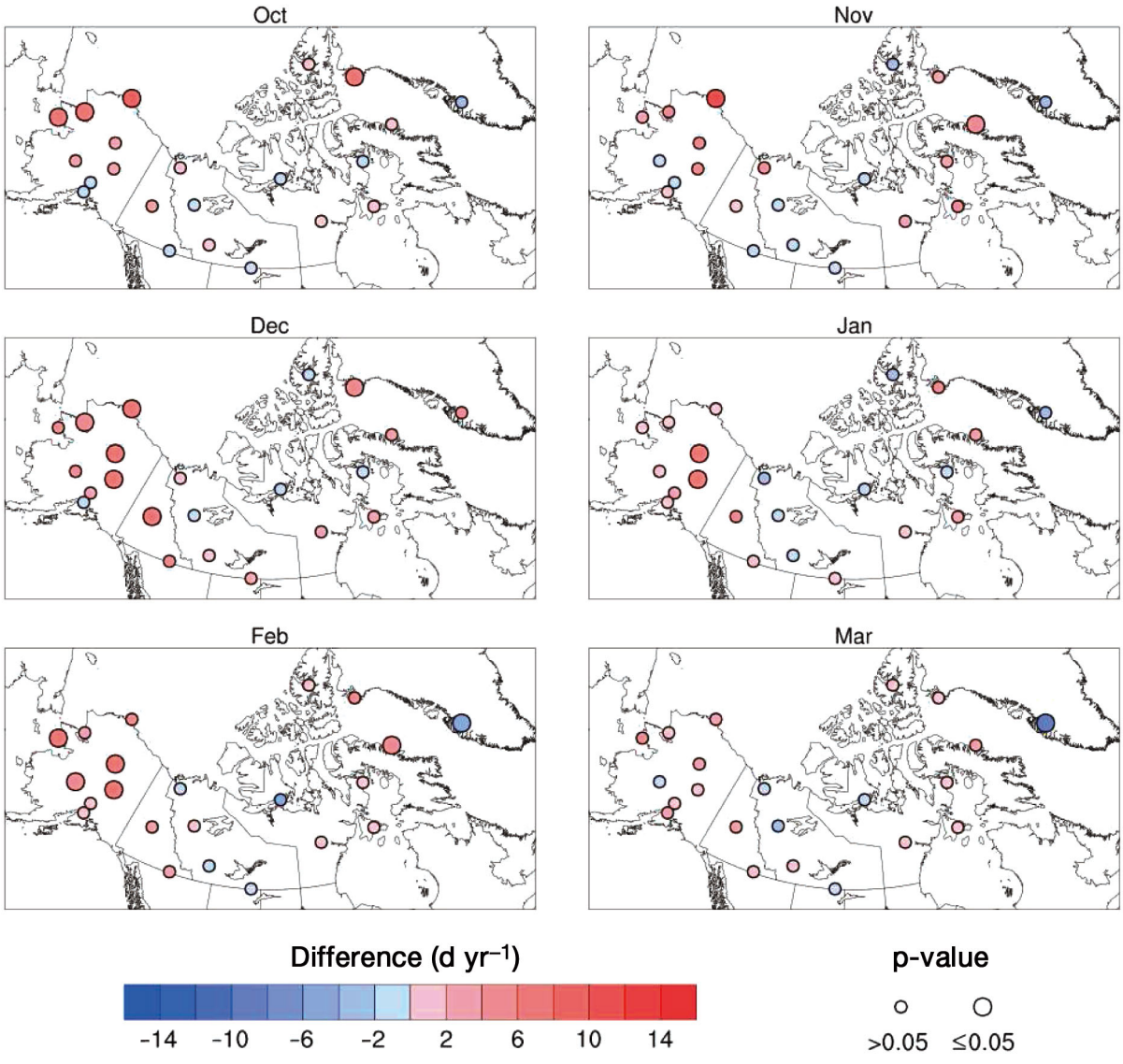

Fig. 10. Monthly differences in Moist Polar classified days and corresponding statistical significance for the late minus early freeze-up years. The difference between the averages of these two 7-yr periods is portrayed in each plot

delays have been linked to large-scale weather type changes in high latitude North America to ~60° N through synoptic environments that support the movement of relatively warm air from the atmosphere overlaying the Beaufort and Chukchi Seas to the NAA. A number of other climatic and environmental factors may also be influencing the anomalous circulation, thereby connecting areas of sea ice decline to high latitude weather patterns. As mentioned in the Introduction, decreasing ice cover in the Barents/Kara and East Siberian/Chukchi seas is believed to be aiding in the amplification of large-scale atmospheric patterns. However, other potentially inter-related climate anomalies including, but not limited to, Eurasian snow cover extent, phases of ocean-atmosphere teleconnections not previously mentioned (e.g. negative Arctic Oscillation/North Atlantic Oscillation), and Atlantic and Pacific sea surface temperature patterns (e.g. Lin & Wu 2012, Mote & Kutney 2012, Cohen et al. 2013, 2014, Hall et al. 2015, Overland et al. 2015, Peings & Magnusdottir 2015) have also been associated with recent changes in atmospheric circulation, which impact North American weather and climate. The linkages between Western Arctic sea ice and NAA surface conditions that are presented in this article provide further evidence that sea ice variability, especially in one portion of the Arctic Ocean bordering the North

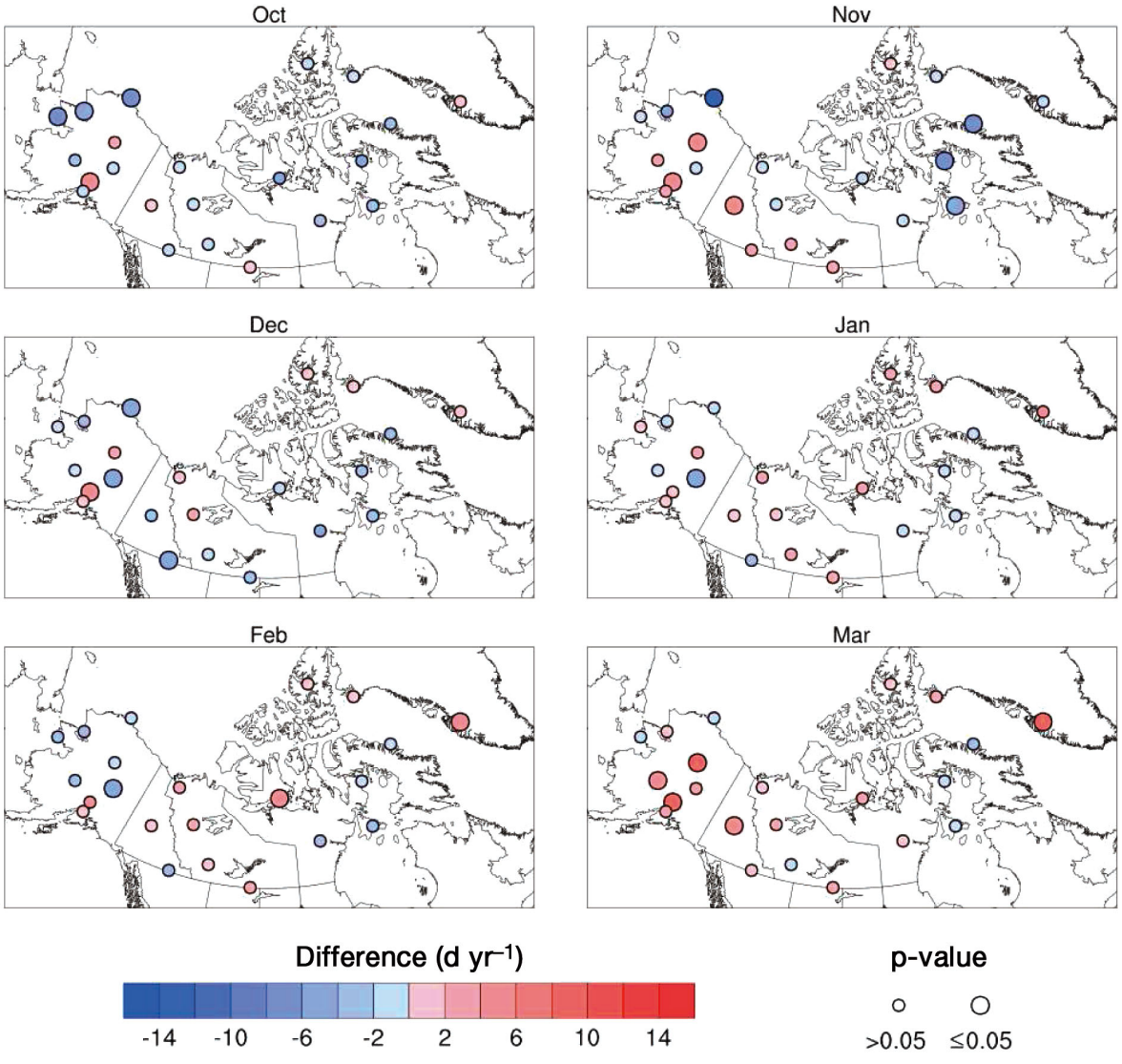

Fig. 11. Monthly differences in Dry Polar classified days and corresponding statistical significance for the late minus early freeze-up years. The difference between the averages of these two 7-yr periods is portrayed in each plot

American continent, may be influencing neighboring, lower latitude climates.

5. CONCLUSIONS

This study presents a novel synoptic climatological approach to further understanding sea ice–climate connections. Monthly trend analyses indicate widespread climatic change in the NAA from colder, drier DP types to relatively warmer, more humid MP types, particularly over Alaska and the Yukon Territory during most months analyzed. These MP frequency changes are positively correlated with the date of the Western Arctic freeze-up, while DP occurrences and ice cover are anti-correlated at similar magnitudes, especially across much of the most northern and western, terrestrial portions of the domain. Composite analyses during extreme freeze-up years further associate MP frequencies with the ice cover behaviors as MP classified days are much more pervasive in the months surrounding the later freeze-up years versus those months where the freeze occurs earlier. Differences in middle and lower tropospheric synoptic fields between late and early years teleconnect recent freeze-up patterns to increases in MP days across a large portion of the NAA.

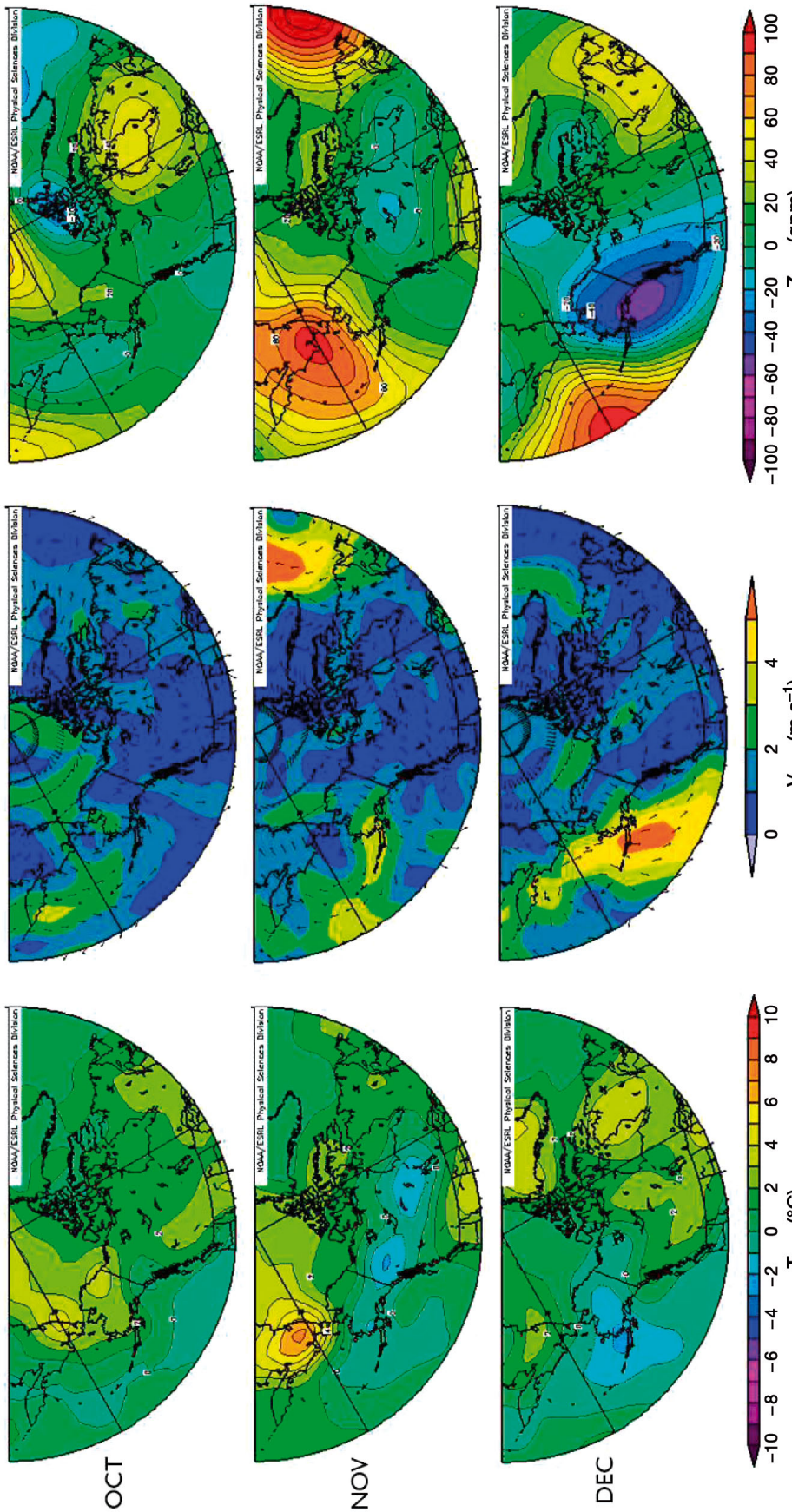

Fig. 12. Composites (late minus early freeze-up years) of 925 hPa air temperature (T_{925}) and vector wind (V_{925}), and 500 hPa geopotential height (Z_{500}) for October to December. gpm: geopotential metres

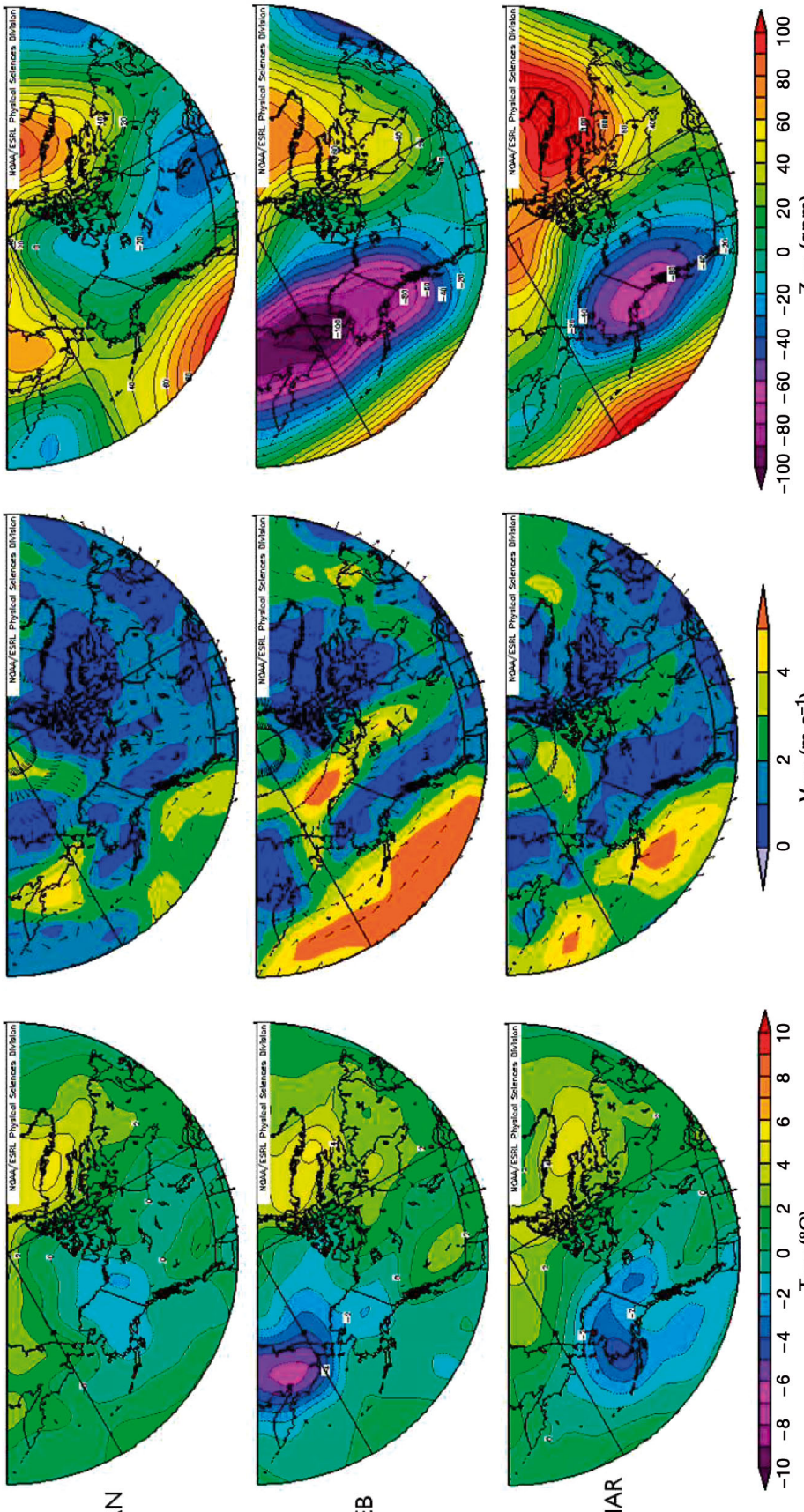

Fig. 13. Composites (late minus early freeze-up years) of 925 hPa air temperature (T_{925}) and vector wind (V_{925}), and 500 hPa geopotential height (Z_{500}) for January to March. gpm: geopotential metres

It is recognized that the freeze-up patterns throughout the Beaufort and Chukchi Seas are variable and therefore portions of each sea may be ice-free for longer or shorter periods each year than the aggregated set of dates used this study. Future research may therefore build upon the results presented here by further evaluating how spatial patterns of freeze onset in the marginal seas affect climate across North America. This may be achieved by evaluating SSC weather-type frequency anomalies farther south, in the more densely configured weather station network of southern Canada and the contiguous United States. Analysis across a broader domain may provide additional insight into the geographic extent of sea ice-weather type relationships as research strives to better understand atmospheric mechanisms potentially linking cryospheric change to middle-latitude extreme events, such as the very cold, snowy winter of 2013/2014 over the eastern and midwestern United States (Palmer 2014).

Acknowledgements. The authors thank Julien Nicolas (Polar Meteorology Group, Byrd Polar and Climate Research Center, The Ohio State University) for assistance writing the scripts used to create several figures found within this manuscript, and Jeffrey Miller (NASA Cryospheric Sciences Laboratory and Wyle) for providing the sea ice dataset and feedback on its description. Comments from Thomas Schmidlin and Mandy Munro-Stasiuk (Kent State University, Department of Geography), and Joseph Ortiz (Kent State University, Department of Geology), and 3 anonymous reviewers also improved this manuscript. The SSC data are obtained from the Spatial Synoptic Classification homepage (http://sheridan.geog.kent.edu/ssc.html), while the freeze-up data are acquired from the NASA Cryosphere Science Research Portal (http://neptune.gsfc.nasa.gov/csb/index.php?section=54). Jeffrey Miller provided the 2012 to 2013 updates for the freeze-up dataset.

LITERATURE CITED

Asplin MG, Fissel DB, Papakyriakou TN, Barber DG (2015) Synoptic climatology of the southern Beaufort Sea troposphere with comparisons to surface winds. Atmos-Ocean 53:264–281

Barnes EA (2013) Revisiting the evidence linking Arctic Amplification to extreme weather in midlatitudes. Geophys Res Lett 40:4734–4739

Barnes EA, Dunn-Sigouin E, Masato G, Woolings T (2014) Exploring recent trends in Northern Hemisphere blocking. Geophys Res Lett 41:638–644

Bekryaev RV, Polyakov IV, Alexeev VA (2010) Role of polar amplification in long-term surface air temperature variations modern Arctic warming. J Clim 23:3888–3906

Bieniek PA, Walsh JE, Thoman RL, Bhatt US (2014) Using climate divisions to analyze variations and trends in Alaskan temperature and precipitation. J Clim 27:2800–2818

Budikova D (2009) Role of Arctic sea ice in global atmospheric circulation: a review. Global Planet Change 68: 149–163

Cassano EN, Cassano JJ, Higgins ME, Serreze MC (2014) Atmospheric impacts of an Arctic sea ice minimum as seen in the Community Atmosphere Model. Int J Climatol 34:766–779.

Cohen J, Jones J, Furtado JC, Tziperman E (2013) Warm Arctic, cold continents: a common pattern related to Arctic sea ice melt, snow advance, and extreme winter weather. Oceanography (Wash DC) 26:150–160

Cohen J, Screen JA, Furtado JC, Barlow M and others (2014) Recent Arctic amplification and extreme mid-latitude weather. Nat Geosci 7:627–637

Dyer JL, Mote TL (2007) Trends in snow ablation over North America. Int J Climatol 27:739–748

Feldstein SB, Lee S (2014) Intraseasonal and interdecadal jet shifts in the Northern Hemisphere: the role of warm pool tropical convection and sea ice. J Clim 27:6497–6518

Francis JA, Chan W, Leather DJ, Miller JR, Veron DE (2009) Winter Northern Hemisphere weather patterns remember summer Arctic sea-ice extent. Geophys Res Lett 36: L07503, doi:10.1029/2009GL037274

Francis JA, Vavrus SJ (2012) Evidence linking Arctic amplification to extreme weather in mid-latitudes. Geophys Res Lett 39:L06801, doi:10.1029/2012GL051000

Francis J, Skific N (2015) Evidence linking rapid Arctic warming to mid-latitude weather patterns. Philos Trans R SocA 373:20140170, doi:10.1098/rsta.2014.0170

Francis JA, Vavrus SJ (2015) Evidence for a wavier jet stream in response to rapid Arctic warming. Environ Res Lett 10:014005, doi:10.1088/1748-9326/10/1/014005

Hall R, Erdélyi R, Hanna E, Jones JM, Scaife AA (2015) Drivers of North Atlantic Polar Front jet stream variability. Int J Climatol 35:1697–1720

Kalnay E, Kanamitsu M, Kistler R, Collins W and others (1996) The NCEP/NCAR 40-year reanalysis project. Bull Am Meteorol Soc 77:437–471

Koenigk T, Caian M, Nikulin G, Schimanke S (2016) Regional Arctic sea ice variations as predictor for winter climate conditions. Clim Dyn 46:317–337

Kug JS, Jeong JH, Jang YS, Kim BM, Folland CK, Min SK, Son SW (2015) Two distinct influences of Arctic warming on cold winters over North America and East Asia. Nat Geosci 8:759–762

Leathers DJ, Mote TL, Grundstein AJ, Robinson DA, Felter K, Conrad K, Sedywitz L (2002) Associations between continental-scale snow cover anomalies and air mass frequencies across eastern North America. Int J Climatol 22:1473–1494

Lin H, Wu Z (2012) Contribution of Tibetian Plateau snow cover to the extreme winter conditions of 2009/2010. Atmos-Ocean 50:86–94

Liptak J, Strong C (2014) The winter atmospheric response to sea ice anomalies in the Barents Sea. J Clim 27:914–924

Liu J, Curry JA, Wang H, Song M, Horton RM (2012) Impact of declining Arctic sea ice on winter snowfall. Proc Natl Acad Sci USA 109:4074–4079

Liu Z, Jian Z, Yoshimura K, Buenning NH, Poulsen CJ, Bowen GJ (2015) Recent contrasting winters over North America linked to enhanced positive Pacific-North American pattern. Geophys Res Lett 42:7750–7757

Markus T, Stroeve JC, Miller J (2009) Recent changes in Arctic sea ice melt onset, freezeup, and melt season length. J Geophys Res 114:C12024, doi:10.1029/2009JC005436

Mori M, Watanabe M, Shiogama H, Inoue J, Kimoto M (2014) Robust Arctic sea-ice influence on the frequent Eurasian cold winters in past decades. Nat Clim Change 7:869–873

Mote TL, Kutney ER (2012) Regions of autumn Eurasian snow cover and associations with North American winter temperatures. Int J Climatol 32:1164–1177

Overland JE, Wang M (2010) Large-scale atmospheric circulation changes are associated with the recent loss of Arctic sea ice. Tellus A 62:1–9

Overland JE, Wood KR, Wang M (2011) Warm Arctic – cold continents: climate impacts of the newly open Arctic Sea. Polar Res 30:15787, doi:10.3402/polar.v30i0.15787

Overland J, Francis J, Hall R, Hanna E, Kim S, Vihma T (2015) The melting Arctic and mid-latitude weather patterns: Are they connected? J Clim 28:7917–7932

Palmer T (2014) Record-breaking winters and global climate change. Science 344:803–804

Peings Y, Magnusdottir G (2015) Role of sea surface temperature, Arctic sea ice and Siberian snow in forcing the atmospheric circulation in winter 2012–2013. Clim Dyn 45:1181–1206

Screen JA, Simmonds I (2013) Exploring links between Arctic amplification and mid-latitude weather. Geophys Res Lett 40:959–964

Serreze MC, Barrett AP, Stroeve JC, Kindig DN, Holland MM (2009) The emergence of surface-based Arctic amplification. The Cryosphere 3:11–19

Serreze MC, Barry RG (2011) Processes and impacts of Arctic amplification: a research synthesis. Global Planet Change 77:85–96

Serreze MC, Barrett AP, Cassano JJ (2011) Circulation and surface controls on the lower troposphere air temperature field of the Arctic. J Geophys Res 116:D07104, doi:10.1029/2010JD015127

Serreze MC, Barrett AP, Stroeve J (2012) Recent changes in tropospheric water vapor over the Arctic as assessed from radiosondes and atmospheric reanalyses. J Geophys Res 117:D10104, doi:10.1029/2011JD017421

Sheridan SC (2002) The redevelopment of a weather-type classification scheme for North America. Int J Climatol 22:51–68

Stroeve JC, Serreze MC, Holland MM, Kay JE, Maslanik J, Barrett AP (2012) The Arctic's rapidly shriking sea ice cover: a research synthesis. Clim Change 110:1005–1027

Stroeve JC, Markus T, Boisvert L, Miller J, Barrett A (2014) Changes in Arctic melt season and implications for sea ice loss. Geophys Res Lett 41:1216–1225

Vihma T (2014) Effects of Arctic sea ice decline on weather and climate: a review. Surv Geophys 35:1175–1214

Wallace JM, Gutzler DS (1981) Teleconnections in the geopotential height field during the Northern Hemisphere winter. Mon Weather Rev 109:784–812

Wendler G, Shulski M, Moore B (2010) Changes in the climate of the Alaskan North Slope and the ice concentration of the adjacent Beaufort Sea. Theor Appl Climatol 99:67–74

Wendler G, Moore B, Galloway K (2014) Strong temperature increase and shrinking sea ice in Arctic Alaska. The Open Atmospheric Science Journal 8:7–15

Wood KR, Overland JE, Salo SA, Bond NA, Williams WJ, Dong X (2013) Is there a 'new normal' climate in the Beaufort Sea? Polar Res 32:19552, doi:10.3402/polar.v32i0.19552

Wood KR, Bond NA, Danielson SL, Overland JE, Salo SA, Stabeno P, Whitefield J (2015) A decade of environmental change in the Pacific Arctic region. Prog Oceanogr 136:12–31

Xia W, Xie H, Changqing K (2014) Assessing trend and variation of Arctic sea-ice extent during 1979–2012 from a latitude perspective of ice edge. Polar Res 33:21249, doi:10.3402/polar.v33.21249

Yarnal B (1993) Synoptic climatology in environmental analysis: a primer. Belhaven Press, London

Editorial responsibility: Oliver Frauenfeld, College Station, Texas, USA

Submitted: June 19, 2015; Accepted: December 6, 2015
Proofs received from author(s): January 28, 2016